Multi-objective optimal design of an organic Rankine cycle plate heat exchanger with phase change

Mahmood Norouzi[1,*], Reza Mahmoodi Targhi[2], Seyyed Majid Hashemian[3], Seyyed Amirreza Vaziri[4], Osman Anwar Beg[5]

[1]Associate Professor, Mechanical Engineering, Shahrood University of Technology, Shahrood, Iran.

[2]M. Sc., Mechanical Engineering, Shahrood University of Technology, Shahrood, Iran.

[3] Assistant Professor, Mechanical Engineering, Shahrood University of Technology, Shahrood, Iran.

[4] Ph. D. Candidate, Mechanical Engineering, Shahrood University of Technology, Shahrood, Iran.

[5] Professor, Aeronautical and Mechanical Engineering, Salford University, Manchester, Uk.

Abstract

In this study, a multi-objective optimization method founded on genetic algorithms is implemented to obtain optimized geometrical parameters for the plate heat exchanger configuration which cause pressure drop minimization and overall heat transfer coefficient maximization. This heat exchanger is basically designed as an evaporator of Organic Rankine Cycles by considering R123 as the working fluid. It is supposed that water vapor with entrance temperature of $150^{\circ}C$ is deployed as hot fluid. A multi-objective optimization method founded on genetic algorithms is implemented to optimize geometrical parameters for the heat exchanger configuration which lead to pressure drop minimization and overall heat transfer coefficient maximization. Two objective functions are conflicting with each other that both single and two-phase flow scenarios are also addressed. In the present optimization method, a Pareto solution is used which permits the derivation of a mathematical relation between the two objective functions simultaneously and yields the optimal geometrical parameters for heat exchangers subjected to constraints associated with the Pareto optimal set. A detailed sensitivity analysis has been conducted for each geometrical parameter and the effects of each parameter on key design characteristics have been evaluated. Both objective function of the

overall heat transfer coefficient and total drop is reduced, by increasing the ports diameter and, due to increasing the thickness of each plate inside the plate heat exchanger, the two-sheet spacing will naturally reduce.

Keywords: Organic Rankine Cycle; Plate heat exchanger; Genetic algorithm; Two-phase flow; Total heat transfer coefficient.

1. Introduction

With considerable growth in global human population, demand for efficient and sustainable energy systems is ever greater. The depletion in primary fossil fuels and energy waste and significant ecological impact associated with these systems have also contributed to tremendous demand for alternative renewable energy design which are clean, cheaper and environmentally-friendly. Electricity generation by burning fossil fuels exerts substantial damage to the planet and it is crucial to increase conversion efficiencies to gain optimum potential of our resources. The sizeable losses incurred via heat transfer from hot surfaces, steam generation losses, leakages, poor insulation and inability to extract complete solar flux have also increased demand for improving thermodynamic efficiencies. There is an ever-growing trend for combined heat and power (CHP) designs in which heat can be recycled and utilized for electrical power [1-4].

An effective technology for this recycling is the Organic Rankine Cycle (ORC), which uses organic fluids as working fluids [5-7]. The thermal energy needed to evaporate the working fluid can be provided by solar thermal collectors. The principal components of ORC-based heat exchangers include turbines (expander) and pumps. Evaporators and condensers have been also deployed as heat exchangers in the cycle and in fact constitute the most critical components of the cycle. Research has demonstrated strongly that heat exchangers in the organic Rankine cycle (evaporator and condenser) contribute exergy losses

of 70% to 90% of the total exergy cycle [8] and 40% to 90% of the capital cost of the cycle. Therefore, the screening, design, and optimization of heat exchangers are fundamental for increasing the overall performance of ORC. Many investigations have been performed on parameter optimization of thermodynamic working fluids and ORC for various applications. Economic criteria, environmental impact and working and production safety are several key factors which contribute to selecting ORC working fluids in low temperature resources [9, 10]. Papadulos *et al.* [11] considered the systematic design and selection of optimal working fluid in an organic Rankine cycle by using the Continuous Approximation of Material Distribution (CAMD) optimization technique, which selects the appropriate fluid via multi-objective optimization. Dai *et al.* [12] investigated the effects of turbine inlet pressure and temperature on the exergy efficiency with a variety of working fluids. They also conducted parametric optimization of ORC by means of GA (genetic algorithms).

Numerous works have also investigated the selection of ORC fluids based on fluid- and process- related properties by testing various available fluids in ORC simulation models [13-15]. Hung *et al.* [16] studied an ORC by using different wet, dry and isentropic fluids. Dry and isentropic fluids showed better thermal efficiencies and moreover, they were observed to not condense during expansion in the turbine, thereby reducing damage and wear during machine operations. Ibarra [17] analyzed the performance of the ORC in part load operation with R245fa and Sdkaterm SES36 working fluids to study the thermodynamic behavior of the elements and determine the best point for each power level. ORC sustains power to 5kW at a maximum temperature of $145^{\circ}C$ by using a scroll expander. The results further demonstrated that the scroll isentropic efficiency has a profound impact on the cycle performance and thermal efficiency and that SES36 generates higher efficiency as a working fluid compared with R245fa. Misra and Roy [18] investigated the performance of two R123 and R134a fluids in ORC systems with regeneration under constant pressure and superheating conditions. In

this study the output turbine efficiency, irreversibility, second law efficiency in the constant state and the variable temperature source were compared and R123 was recommended as the premier fluid. Wang *et al.* [19], compared the relative performance of thirteen different working fluids. Employing simulated refrigeration of the elements, they optimized the ORC parameters and compared the effects of changes in the source temperature and the difference in the pinch temperature on the performance to attain optimum cost. The results indicated that R123 is the best fluid for heat source at temperatures between 100 ℃ to 180 ℃ and R141b is the most appropriate fluid for temperatures above 180 ℃. They also determined that the optimum pinch temperature difference should be set at 15℃. Mago *et al.* [20] presented a second law analysis for the use of ORC to convert low-grade heat to power. They found R123 shows the best efficiency for heat source temperatures between 380 and 430 K. Yari *et al.* [21], Huijuan *et al.* [22] and Roy *et al.* [23] studied the operation of fluids in an ORC and concluded that R123 fluid is a desirable and suitable fluid compatible with the thermodynamic cycle structure and efficiency of the ORC and is therefore the optimal working fluid.

Many studies have focused on the parametric and structural optimization of ORC involving different variables and considering different objectives. Wang *et al.* [24] presented a design method for plate heat exchangers (PHEs) with and without pressure drop specifications. Full utilization of allowable pressure drop was elected as the design objective, in the case of design with pressure drop specification. In the case of no pressure drop specification, allowable pressure drops were determined through economical optimization. Karellas *et al.* [25] investigated the influence of the ORC parameters on the heat exchanger design for supercritical thermodynamic conditions. They concluded that the increase in efficiency is proportionated with cost increasing, and the selection of fluid in the supercritical mode is a very convenient and effective mode of operation. Yan *et al.* [26] studied the heat

transfer and pressure drop in a plate heat exchanger with R134a fluid. They evaluated the effects of refrigerant mass flow, average mass flux, system pressure and steam quality of R134a showing that in the higher steam quality, heat transfer coefficient and pressure drop are significantly higher than the increasing of refrigerant mass flow which induces only a slight increase in the amount of heat transfer coefficient and pressure drop. Accordingly, some relations were presented for the heat transfer coefficients and the pressure drop in terms of Nusselt number (wall heat transfer rate) and friction coefficient. Vaziri *et al.* [27] presented new analytical formulation for an axisymmetric thick-walled functionally graded material cylinder with power-law variation in mechanical and thermal properties under transient heating using first order shear deformation theory that their methodology and FG materials are useful for heat-exchanger optimization. Walraven *et al.* [28] optimized and compared shell-and-tube and plate heat exchangers in an ORC, although their study was limited by a single objective evaluation of the exergy efficiency. The results indicate that plate heat exchangers have a better performance in this cycle.

In recent years, several solutions have been used to optimize processes in the energy industry. One very popular method which has been adopted widely is that of genetic and evolutionary algorithms [29, 30]. Specifically, genetic algorithms (GA), by virtue of their customizable characteristics, are an appropriate method to deal with multi-objective optimization problems [23]. Many studies have been conducted in the optimization of the structure and equipment of the Rankine cycle (especially on heat exchangers) with computer codes based on genetic algorithms [31-33]. Wang *et al.* [34] focused principally on a multi-objective optimization of a plate heat exchanger working as an ORC condenser. The optimization objectives selected were the pressure drop and heat transfer of surface area. In a subsequent study, a multi-objective optimization of the whole ORC was presented. Hilbert *et al.* [35] considered heat exchange and pressure drop as objectives and performed multi

objective optimization to find the optimum geometry which can satisfy both objectives to a desirable level. Najafi et al. [36] investigated the multi-objective optimization (with genetic algorithms) of a plate heat exchanger by optimizing geometric parameters, permitting the determination of the lowest amount of pressure drop and maximum total heat transfer coefficient. In this method of optimization, the Pareto solution was used to establish a relationship between the objective functions and provided several geometric parameters in the presence of constraints, which were assumed as the best solution. Further studies of genetic algorithm-based and neural network multi-objective optimization of thermodynamic cycles have been communicated by Rashidi *et al.* [37] and Bég *et al.* [38].

In the present article, a plate heat exchanger (PHE) is modeled with multi-objective optimization via a genetic algorithm to obtain the optimal geometric parameters which minimizes the pressure drop and maximizes the total heat transfer coefficient. Consequently, a set of optimal solutions based on a Pareto solution is presented which optimizes the two objective functions of heat transfer and pressure drop. R123 and vapor water at temperature 150℃ have been deployed as the working fluid in the ORC (cold fluid at evaporator entrance) and as a heat source respectively. The optimization of the plate heat exchanger and its optimal structure, such as an evaporator in an organic Rankine cycle (organic fluid), have been investigated in both single-phase and two-phase flows. Therefore, the calculations have been carried out by considering that in the cold evaporator fluid and within each layer of the plate heat exchanger, there are three liquid states i.e. two phases and vapor. The calculations have been done for all three modes, and finally the optimal structure of the desired converter has been determined.

2. Description of the organic Rankine cycle (ORC)

The schematic diagram (plan) of the ORC examined in this study is given in **Fig. 1**. The basic ORC consists of a pump which pressurizes the working fluid and directs over to the evaporator. In the evaporator the working fluid is heated to the vapor saturated point and then the working fluid expands through the turbine and produces mechanical work. This shaft power is then converted to electricity by the generator.

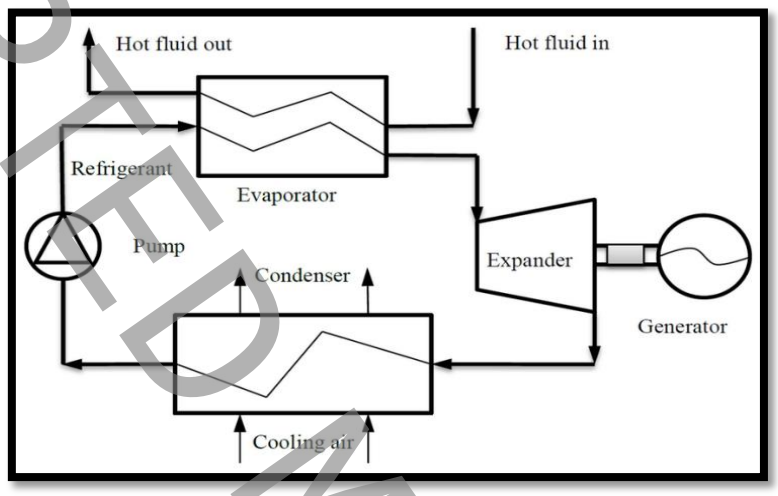

Fig. 1. Schematic of the Organic Rankine Cycle

3. Plate heat exchanger

A plate heat exchanger is assumed as the evaporator in organic Rankine cycle due to high efficiency and compact structure. The plate heat exchangers are fabricated of thin plates that form the flow channels. In the ORC system, the evaporator is a very important component which can influence the overall system performance with respect to the heat sink of the thermodynamic cycle [34]. A plate heat exchanger uses an evaporator in the organic Rankine cycle because of its high efficiency. Fig. 2 illustrates the geometric characteristics of the plate heat exchanger.

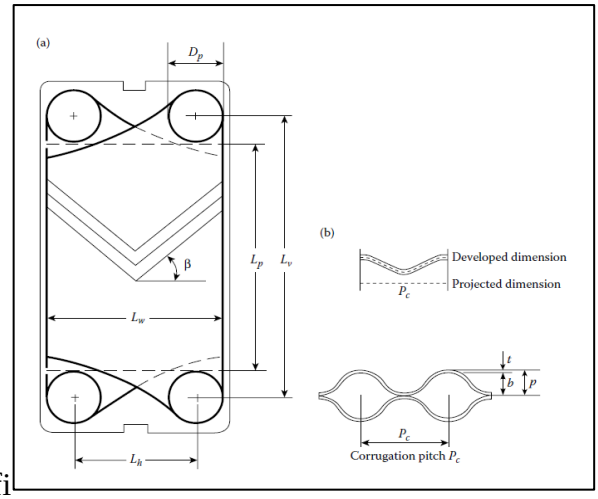

fi

Fig. 2. Geometric characteristics of plate heat exchanger

R123 is selected as the working fluid in the ORC due to its good thermodynamic properties and low environmental impacts and water is used to heat the fluid R123 in the evaporator.

4. Plate heat exchangers equations

To simplify the theoretical models of the PHE, a set of assumptions is introduced in the following:

1- Heat losses to or from the surroundings and kinetic and potential energy changes are negligible.

2- Fouling effects are negligible.

3- The heat exchanger operates under steady-state conditions.

The heat transfer processes for single-phase flow and two-phase flow are respectively discussed next. First, plate heat exchangers geometrical equations are formulated. Then, for each of the two-phase and single-phase cases in the heat exchanger, the equations for heat transfer and pressure drop in each section are presented.

5. Geometric equations for heat exchangers

The length ratio of the PHE is defined as follows with reference to **Fig. 2**:

$$\varnothing = \frac{\text{Developed length}}{\text{Projected length}} = \frac{A_1}{A_{1p}} \tag{1}$$

Here, A_1p can be found using:

$$A_{1p} = L_w L_p \tag{2}$$

Further:

$$L_w = L_h + D_p \tag{3}$$

$$L_p = L_v - D_p \tag{4}$$

The mean flow channel gap, b, can be determined using the following relations:

$$D_e = \frac{2b}{\varnothing} \tag{5}$$

$$b = p - t \tag{6}$$

$$p = \frac{L_c}{N_t} \tag{7}$$

5.1. Single-phase heat transfer and pressure drop

The heat transfer rate is given by:

$$Q = \dot{m} C_p \Delta T \tag{8}$$

Here, $\dot{m}$ is mass flow rate (kg/s), C_p is specific heat capacity (J/kgK) and ΔT is temperature difference (K). The Reynolds number is defined by the mass velocity in the channel (G_{ch}) and the channel diameter (D_e):

$$Re_{ch} = \frac{G_{ch} D_e}{\mu} \tag{9}$$

$$G_{ch} = \frac{\dot{m}}{N_{cp} * A_f} \tag{10}$$

$$N_{cp} = \frac{N_t - 1}{2N_p} \tag{11}$$

where N_t and N_p specify number of plates and number of passes, respectively and μ denotes the dynamic viscosity of the working fluid (kgm/s). A popular method which is used for the heat transfer coefficient (Nusselt Number) calculations in plate and frame heat exchangers is presented by Martin [39]:

$$Nu = 0.205 Pr^{1/3} \left(\frac{\mu_b}{\mu_w}\right)^{1/6} \left(f_{pc} Re^2 \sin 2\beta\right)^{0.374} \tag{12}$$

Here, μ_b is the bulk fluid dynamic viscosity, μ_w is the dynamic viscosity of the fluid at the wall and β is the inclination of a plate to the horizontal. The difference between these viscosities is neglected. *Pr* designates the key thermofluid property parameter in heat transfer i.e. Prandtl number. For a single plate with f_{pc} the Fanning friction factor is given by [40]:

$$\frac{1}{\sqrt{f_{pc}}} = \frac{\cos\beta}{\left(0.045\tan\beta + 0.09\sin\beta + \frac{f_0}{\cos\beta}\right)^{0.5}} + \frac{1-\cos\beta}{\sqrt{3.8 f_1}} \tag{13}$$

Here, f_0 is the Fanning friction coefficient if β =0 and f_1 is the Fanning friction coefficient if $\beta = 1$. These coefficients are given respectively (with the appropriate range of Reynolds numbers) by:

$$f_0 = \begin{cases} \frac{16}{Re} & Re < 2000 \\ \left(1.56\,Ln\,Re - 3\right)^{-2} & Re \geq 2000 \end{cases} \tag{14}$$

$$f_1 = \begin{cases} \dfrac{149.25}{Re} + 0.9625 & Re < 2000 \\ \dfrac{9.75}{Re^{0.289}} & Re \geq 2000 \end{cases} \quad (15)$$

The convection heat transfer coefficient for the single-phase flow case is expressed as:

$$h = \frac{Nu\, k_f}{D_e} \quad (16)$$

Here, k_f denotes the working fluid thermal conductivity (W/mK) and h has units of (W/K).

The total pressure drop is composed of the frictional channel pressure drop, Δp_{ch}, and the port pressure drop, Δp_p. The first component, Δp_{ch}, is defined by the following equation [36]:

$$\Delta p_{ch} = 4 f \left(\frac{L_{eef} . N_p . G_{ch}^{\ 2}}{2 D_e . \rho} \right) . \left(\frac{\mu_b}{\mu_w} \right)^{-0.17} \quad (17)$$

where ρ is the fluid density (kg/m^3) and the friction factor, *f*, is defined by the following equation for the frictional pressure drop:

$$f = \frac{k_p}{Re_{ch}^{\ m}} \quad (18)$$

The pressure drop in the port ducts is expressed as [36]:

$$\Delta p_p = 1.4 N_p \frac{G_p^{\ 2}}{2\rho} \quad (19)$$

$$G_p = \frac{4\dot{m}}{\pi D_p^{\ 2}} \quad (20)$$

As a result, the overall pressure drop in the single-phase mode is as follows:

$$\Delta p_{sp} = \Delta p_p + \Delta p_{ch} \tag{21}$$

It is important to note that working fluids here are assumed to be stable, non-fouling, non-corrosive, non-flammable and non-toxic, all desirable features for safe ORC systems.

5.2. Two-phase heat transfer and pressure drop

Han *et al.* [41] developed correlations for the pressure drop and heat transfer in Chevron-type plate heat exchangers during evaporation. The heat transfer coefficient is correlated as:

$$Nu = C_1 \left(Re_{eq}^{\ C_2} \right) \left(Bo_{eq}^{\ 0.3} \right) \left(Pr^{0.4} \right) \tag{22}$$

where

$$C_1 = 2.81 \left(\frac{b}{De}\right)^{-0.041} \beta^{-2.83} \tag{23}$$

$$C_2 = 0.746 \left(\frac{b}{De}\right)^{-0.082} \beta^{0.61} \tag{24}$$

$$Re_{eq} = \frac{G_{eq} D_e}{\mu_1} \tag{25}$$

$$Bo_{eq} = \frac{\dot{q}}{G_{eq} \gamma} \tag{26}$$

Here, Bo_{eq} is the equivalent boiling number. Also, G_{eq} is the equivalent mass velocity, defined as [41]:

$$G_{eq} = G \left[(1-x) + x \left(\frac{\rho_1}{\rho_g} \right) \right] \tag{27}$$

where x is the vapor quality for each section and $\rho_l$and ρ_g are the densities of saturated liquid and saturated vapor, respectively. The frictional pressure drop in one plate during evaporation is:

$$\Delta p_{fr} = 4\left[\frac{f_{fr} L_p}{D_e} \frac{G_{eq}{}^2}{2\rho_l}\right] \tag{28}$$

The correlation for the Fanning friction factor is given by:

$$f_{fr} = C_3 Re_{eq}{}^{C_4} \tag{29}$$

where

$$C_3 = 64710\left(\frac{p}{D_e}\right)^{-5.27} \beta^{-3.03} \tag{30}$$

$$C_4 = 64710\left(\frac{p}{D_e}\right)^{-0.62} \beta^{-0.47} \tag{31}$$

The acceleration pressure drop is given by[41]:

$$\Delta p_a = \left[\frac{G_{eq}{}^2 x}{(\rho_l - \rho_v)}\right]_{out} - \left[\frac{G_{eq}{}^2 x}{(\rho_l - \rho_v)}\right]_{in} \tag{32}$$

As a result, the overall pressure drop in the single-phase regime is as follows:

$$\Delta p_{tp} = \Delta p_{fr} + \Delta p_a \tag{33}$$

Finally, the total pressure drop (evaporator) as a function of the objective function is obtained from the following equation:

$$\Delta p_{tot} = \Delta p_{sp} + \Delta p_{tp} \tag{34}$$

It follows that the total heat transfer coefficient (objective function) is as follows:

$$U = \left(\frac{1}{h_c} + \frac{1}{h_h} + \frac{t}{k_w}\right)^{-1} \tag{35}$$

6. Optimization procedure

A genetic algorithm is used here to solve the optimization problem. This approach was pioneered by American physicist and computer scientist, Holland [29] in the mid-1970s. The genetic algorithm has been developed on the basis of natural selection theory in biological genetic advancements, which differs from traditional methods of optimization, since it involves searching for a solutions of populations, not from a single point, which prevents the convergence of the sub-optimal solutions in the desirable search process, and can also solve the problem of complex optimization, such as non-linear or discrete problems as elaborated by Mitchell [42]. Genetic algorithms are based on evolutionary theory and the problem solved by the genetic algorithm is continuously improved. The genetic algorithm begins with a set of answers that are shown through the chromosomes. This set of answers is termed the primitive population. In this algorithm, responses from a population are used to generate the next population. In this process, it is hoped that the new population would be better than the previous population. Choosing some of the answers from the total answers (parents) to give new answers to the children is based on their desirability. It is natural that the appropriate answers have a greater chance of reproduction. This process continues until a predetermined condition (such as the number of populations or the rate of improvement) occurs. This procedure has been shown in fig. 3.

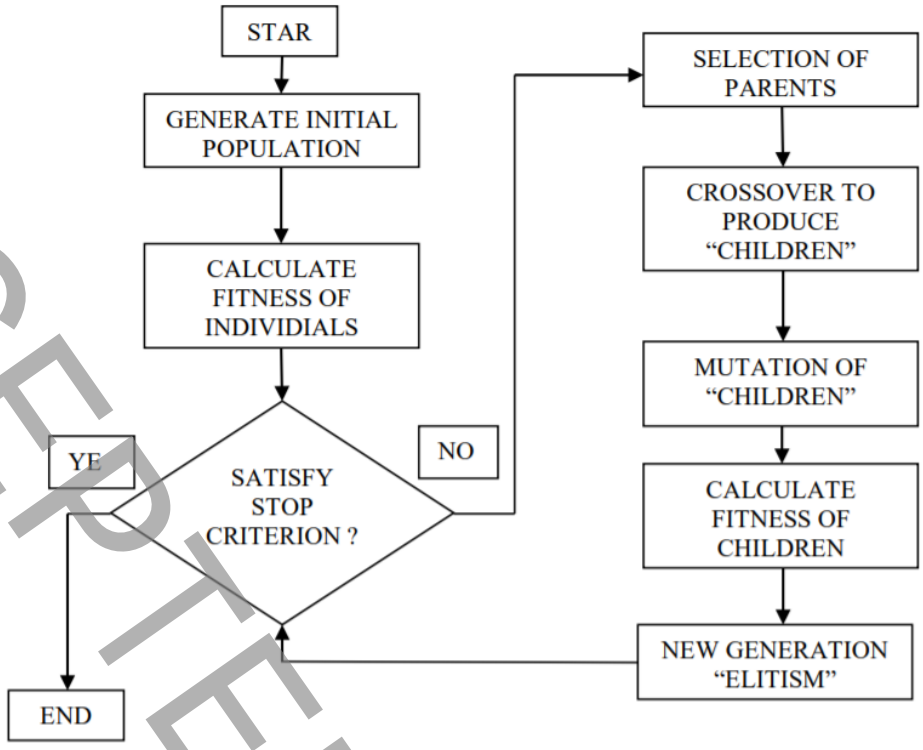

Fig. 3 Flow chart of the Matlab Genetic Algorithm

The evaporator operating condition (functional condition) expressed in **Table 1**.

Table. 1. Evaporator operating condition.

Operating condition	**Hot Side**	**Cold Side**
Fluid	Steam	R123
PHE inlet temperature (°C)	150	30
PHE outlet temperature (°C)	122	80
Pressure (bar)	1	2
Mass flow rate (kg/s)	0.3	0.09

According to the fundamental premise of the genetic algorithm, it is needed to consider the independent variables for optimizing the plate heat exchanger to be optimized using the fitness function (objective). Since the overall heat transfer coefficient should be maximized, -*U* is considered as one of the objective functions and is minimized through the optimization procedure which in turn leads to maximization of the overall heat transfer coefficient (*U*). In each iteration, the values of optimization parameters (including port diameter, total number of plates, vertical and horizontal lengths of the plate and the plate thickness) are changed and then the considered objective functions are evaluated based on the new values.

Table. 2. Optimization parameters: constant values and corresponding constraints

Parameter	**Constant value**	**Considered range**
Plate thickness, $\boldsymbol{t}$ (m)	0.0006	0.0003 – 0.001
Diameter of ports, $\boldsymbol{D_p}$ (m)	0.073	0.03 – 0.15
Vertical distance of ports, $\boldsymbol{L_v}$ (m)	0.620	0.3 – 1.1
Horizontal distance of ports, $\boldsymbol{L_h}$ (m)	0.15	0.15 – 0.5
Number of plate	31	10 - 60
Number of passes	1	Constant

Thermal conductivity of plates ($\mathbf{W/mK}$)	17.11	Constant
Chevron angle (D)	60	Constant
Enlargement factor , $\emptyset$	1.25	Constant

According to the **Table 2**, five geometric parameters have defined as the optimization parameter, each of one has a certain (specific range) limitation for optimization that heat exchanger design should be in this range. Due to the cold fluid flow (R123) inside the evaporator, the fluid phase changes over the plate, so heat transfer calculations, especially the calculation of the convention heat transfer coefficient (h), are difficult to calculate. The averaging method is used to calculate the convention heat transfer coefficient of cold evaporator fluid, which can be used as following:

$$\overline{h_c} = \frac{1}{A}\int h_c \, dA \tag{36}$$

By substituting $\overline{h_c}$ in Eqn. (3), the total heat transfer coefficient (U) can be obtained.

7. Validation

To validate the present computations, the reported results by Kakac [43] and Najafi *et al.* [31] compared with results produced by the Aspen EDR heat exchanger design software [39]. In work of Kakac [43], the procedure of design of plate heat exchanger is explained in detail. Najafi *et al.* [31] used exactly the same procedure and operating conditions to obtain the optimal design. In both works of Najafi *et al.* [31] and Kakac [43], the water is considered as cold and hot fluid. The operating conditions and geometry of plate heat exchanger are also reported in Tables 3 and 4. They obtained the pressure drop and overall heat transfer coefficient as 592010 Pa and 9926.5 W/ $\boldsymbol{m^2}$ **K**, respectively. These results correlate closely

with solutions generated from the thermodynamic model used in this paper with error less than 1%.

Table 3. Operating conditions in work of Kakac [43] and Najafi *et al.* [31]

Parameter	Hot Side	Cold Side
Mass flow rate (kg/s)	140	140
PHE inlet temperature (°C)	65	22
PHE outlet temperature (°C)	45	42
Pressure (bar)	1	2
Specific heat of fluid ($^{J}/_{KgK}$)	4138	4178
Viscosity ($^{Ns}/_{m^2}$)	0.000509	0.000766
Thermal conductivity coefficient ($^{W}/_{mK}$)	0.645	0.617
Density ($^{kg}/_{m^3}$)	985	995

Table 4. Geometry of plate heat exchanger in work of Kakac [43] and Najafi *et al.* [31]

Parameter	Constant value
Plate thickness, t (m)	0.0006
Diameter of ports D_p, (m)	0.2
Vertical distance of ports, L_v (m)	1.55
Horizontal distance of ports, L_h (m)	0.43
Enlargement factor **(∅)**	1.25
Number of passes	1
Thermal conductivity of plates (W/mK)	17.11
Chevron angle (D)	60
Number of plate	105

Finally, to ensure the reliability of the used method, the results of the present study have been compared to Aspen EDR software by using the functional conditions and the fixed values of Tables 1 and 2. The objective functions have been obtained in Aspen EDR software according to Table 5. According to the Table 5, the overall heat transfer coefficient and total pressure drop obtained in this study have a consistent agreement. Therefore, with regard to validation, it can be seen that the relationships between the present research and the method used to solve the problem have acceptable accuracy. The small deviation between the results could be attributed to use of the different empirical correlations to estimate the Nusselt number and Fanning friction coefficient.

Table. 5. Validation with Aspen Software

Objective Functions	Present study	Aspen Software	Error $\%$
U $(\mathbf{W/m^2 K})$	197.4	204.5	3
Δp_t (Pa)	46542	51078	8

8. Results and discussion

8.1. Sensitivity analysis

Sensitivity analysis involves investigation of the effect of selected design variable values on considered objective functions. The influence of each design parameter in a distinct geometry and reasonable range (according to the **Table 2**) is examined on two objective functions i.e. the total heat transfer coefficient and total pressure drop in the plate heat exchanger. In addition, in this analysis, functional conditions are used according to **Table 1**.

8.1.1. Ports diameter (D_p)

The diameter augmentation of the ports on each plate of the heat exchanger, as shown in **Fig. 4**, leads to a decrease in the overall heat transfer coefficient. This is attributable to the fact that according to the energy equation, the velocity of the fluid decreases and finally the heat transfer coefficient is decreased. As the diameter of the ports increases, the area of the flow inside the ports increases. Effectively therefore, the fluid velocity is decreased and eventually this manifests in a non-trivial pressure drop.

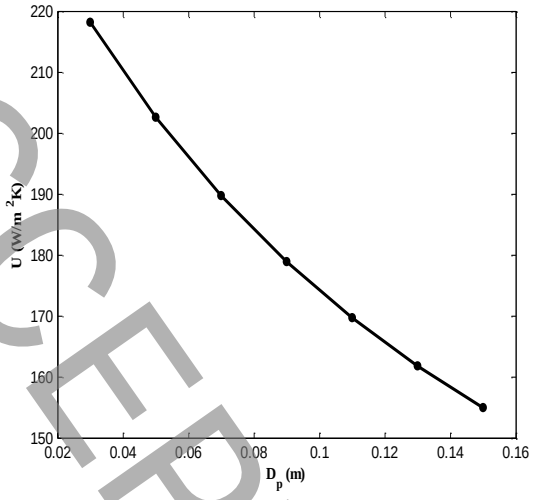

(a)

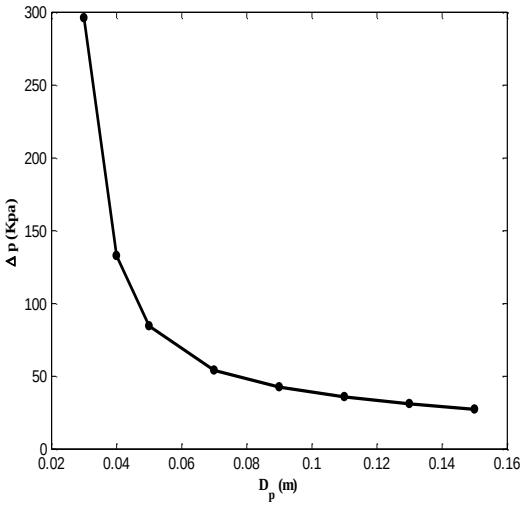

(b)

Fig. 4 (a): Effect of plate's Ports diameter (D_p) on total heat transfer coefficient and (b): Effect of plate's Ports diameter (D_p) on total pressure drop

8.1.2. Plates thickness

With respect to Figs. 5 (a) and 5 (b), both the total pressure drop and the overall heat transfer coefficient are enhanced by increasing the thickness of the plates.

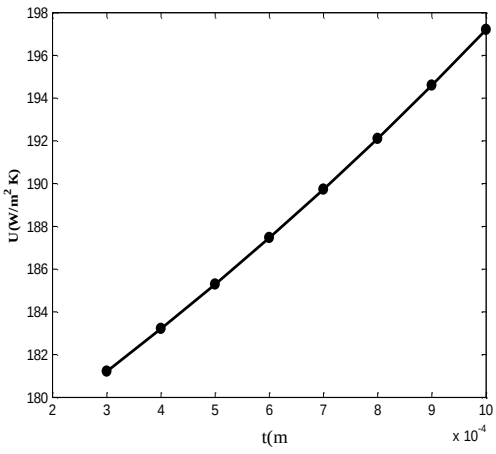

(a)

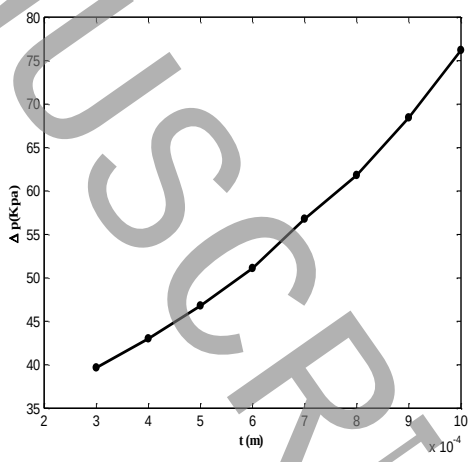

(b)

Fig. 5 (a) Effect of plates thickness (*t*) on total heat transfer coefficient and (*b*) Effect of plates thickness (*t*) on total pressure drop

By increasing the plates thickness, the average distance between the flow channels decreases and therefore reduces the heat transfer surface and ultimately leads to an augmentation in the overall heat transfer coefficient. Thermal conduction heat transfer in the solid plates probably also contributes to this. In Fig. 5 (*b*), augmentation of plates thickness and decreasing the area of the channel results in acceleration in the flow and eventually leads to an augmentation in the pressure drop in the heat exchanger.

8.1.3. The port horizontal distance

Increasing the horizontal distance (L_h) of the ports leads to an increase in the surface area of each plate. This in turn raises the average channel flow distance which subsequently reduces the overall heat transfer coefficient and decreases overall pressure drop, as depicted in **Figs. 6a** and **6b**.

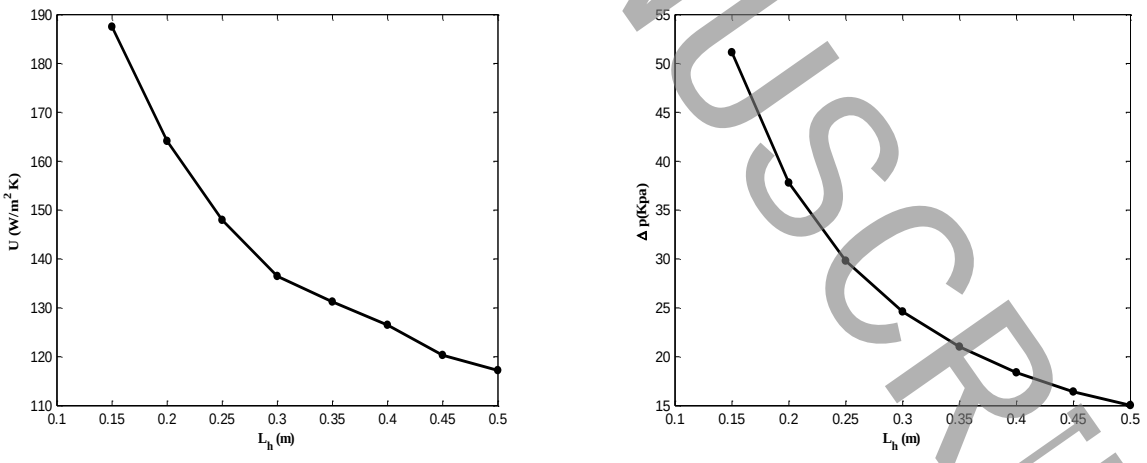

(a) (b)

Fig. 6. (a): Effect of plate's ports horizontal distance (L_h) on total heat transfer coefficient and (b): Effect of plate's ports horizontal distance (L_h) on total pressure drop

8.1.4. The port vertical distance

In the previous section, the distance between the ports could be changed at the heat transfer surface. According to Fig. 7 (a), the heat transfer coefficient decreases by increasing the vertical distance of the ports (L_v), as in the previous section. This is due to accentuation of the heat transfer surface. However, in Fig. 7 (b), in contrast to the horizontal distance of the ports, the pressure drop increases with increasing port vertical distances. This is induced due to the fluid flow direction in the vertical direction and the associated flow path enhancement with increasing vertical distances of the ports. Increasing the pressure drop (especially the frictional pressure drop component) is the net effect in heat exchangers.

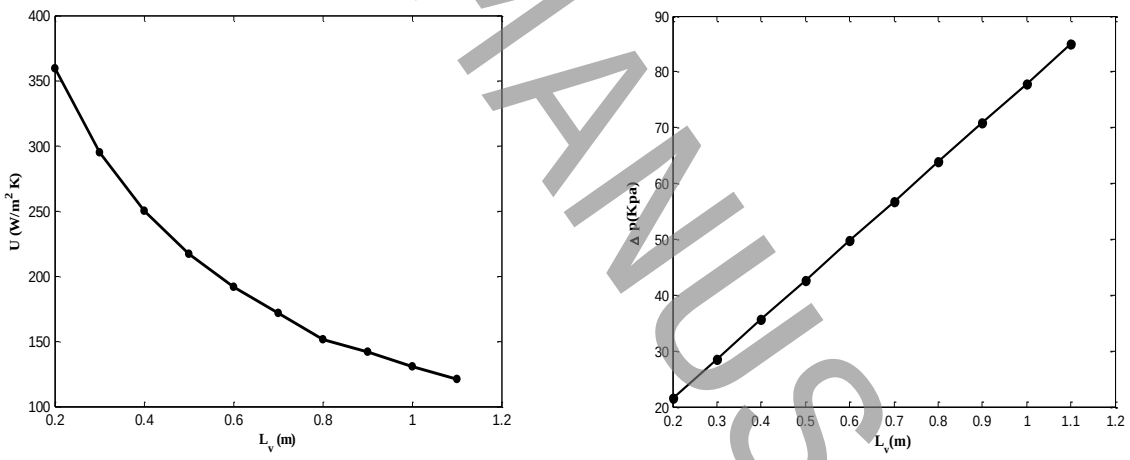

(a) (b)

Fig. 7. (a): Effect of plate's the ports vertical distance (L_v) on total heat transfer coefficient and (b): Effect of plate's the ports vertical distance (L_v) on total pressure drop

8.1.5. Number of plates (N_t)

As shown in **Figs.** 8 (a) and 8 (b), with increasing number of plates, the total heat transfer coefficient and total pressure drop of both plates decrease. As the number of plates in the evaporator increases, the number of flow channels increases. Therefore, the velocity of the fluid in the channels decreases and finally the pressure drop and the total heat transfer coefficient are reduced.

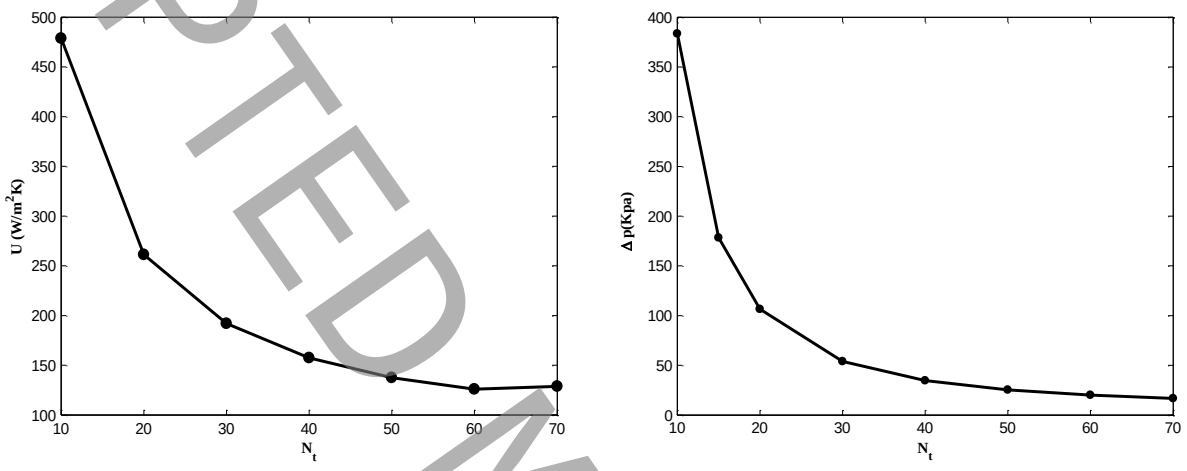

(a) (b)

Fig. 8. (a): Effect of number of plate (N_t) on total heat transfer coefficient and (b): Effect of number of plate (N_t) on total pressure drop

8.2. Multi-objective optimization results

8.2.1. Working fluid flow rates (R123)

Multi-objective optimization by using genetic algorithms is applied to a heat exchanger plate in order to find optimum geometric parameters. In this paper, the optimization of heat

exchanger plates in an organic Rankin cycle using different working fluid flow rates (R123) under the operating conditions of **Table 2** and the geometric conditions of **Table 1** have been considered. The parameter design and the objective function values for a specific working fluid flow rate evaluated by the genetic algorithm are shown in **Table 6**.

Table. 6. Selected results of the generated Pareto front for $\dot{m} = 0.5\ kg/s$.

U (W/ m^{2}K)	Δp (kPa)	N_t	L_v(m)	L_h(m)	t(m)	D_p(m)
571.32	87.970	18	0.744	0.156	0.000882	0.060
561.2	70.053	22	0.710	0.215	0.000916	0.0722
543.26	55.34	25	0.700	0.241	0.00071	0.0971
523.24	44.259	27	0.671	0.25	0.00087	0.0827
489.34	37.901	34	0.548	0.307	0.00061	0.123
478.52	34.248	38	0.693	0.267	0.00088	0.0824
361.58	20.916	41	0.772	0.297	0.00054	0.0926
341.37	17.357	48	0.681	0.314	0.00056	0.0961
237.10	9.846	54	0.449	0.412	0.00049	0.127
155.34	3.102	60	0.457	0.499	0.00032	0.15

In **Table 6**, data is provided for 10 series of optimal results produced by the Pareto solution for $\dot{m} = 0.5$ kg/s. In **Fig. 9,** the Pareto charts corresponding to various flow rates is presented.

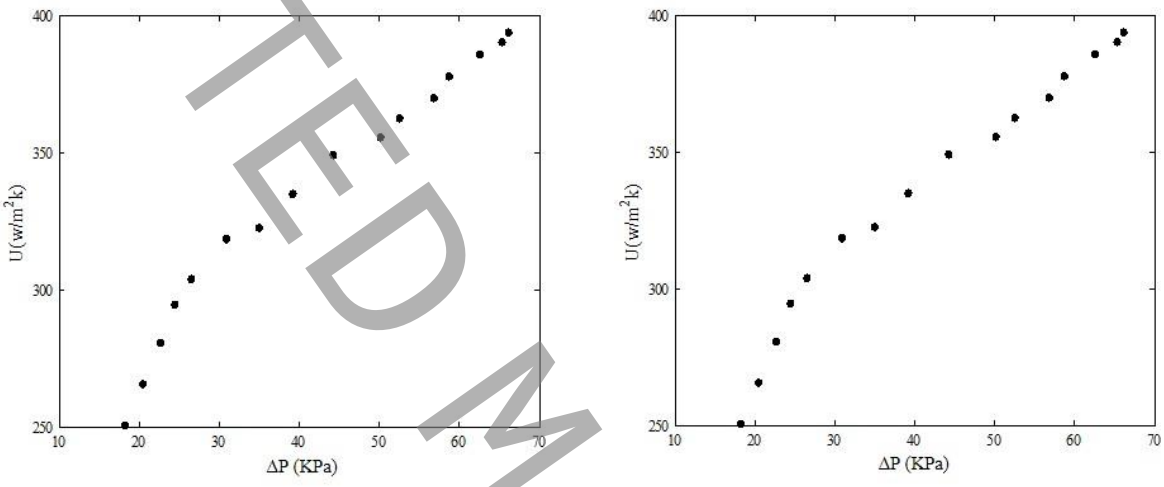

(a) (b)

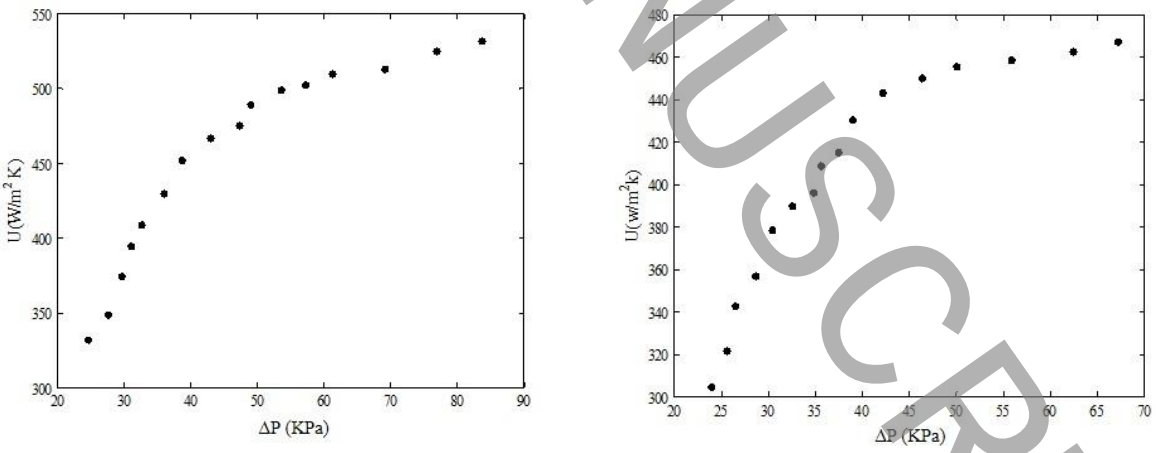

(c) (d)

Fig. 9. Generated Pareto front for (a) $\dot{m} = 0.09$ kg/s, (b) $\dot{m} = 0.5$ kg/s, (c) $\dot{m} = 1$ kg/s, and (d) $\dot{m} = 1.5$ kg/s.

According to the Pareto graphs, 16 optimal modes have been obtained for the working fluid flow rates that can be used to select optimal design parameters using various constraints and conditions. As mentioned earlier, with increasing working fluid mass rate, the overall heat transfer coefficient and overall pressure drop increase so there is a need to present a solution for reduction of pressure drop and optimize the heat exchanger. In the previous section (sensitivity analysis), among the design parameters the major impact is related to the numbers of plates. Hence the appropriate choice of plate numbers can have a significant effect on heat exchanger optimization. Based on the given data, it is evident that with increasing fluid mass rate, the plate numbers for the optimum case will increase. Finally, with increasing plate numbers, the overall heat exchanger pressure drop decreases and the optimum case for heat exchangers may be achieved.

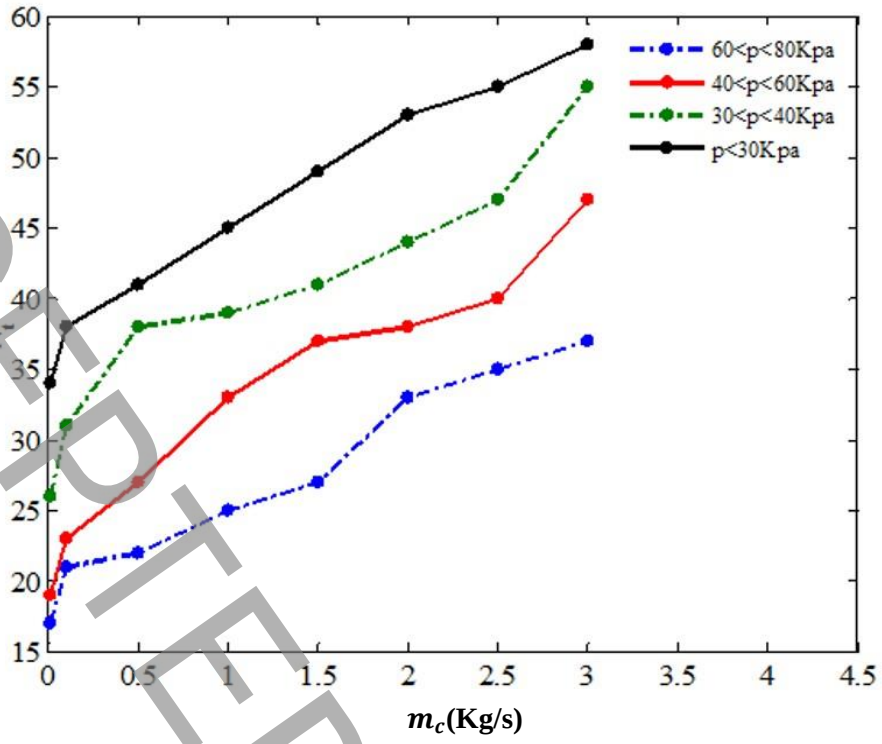

Fig. 10. Effect of working fluid mass rate (R123) on plate numbers in heat exchangers optimization using genetic algorithm

For each of working fluid mass rates, four optimum states have been given from high pressure drop to low pressure drop, respectively. With regard to **Fig.** 10 which is a result of optimization, it can be observed in every expressed pressure drop interval, that with increasing working fluid mass rate, the number of heat exchanger plates will increase to prevent further pressure drop. Moreover, if the drop pressure interval is assumed to be large then lower plate numbers will be needed. Subsequently in this case, heat transfer coefficient will be higher. Therefore, for optimization purposes in low pressure drop, it is necessary to increase the plate numbers.

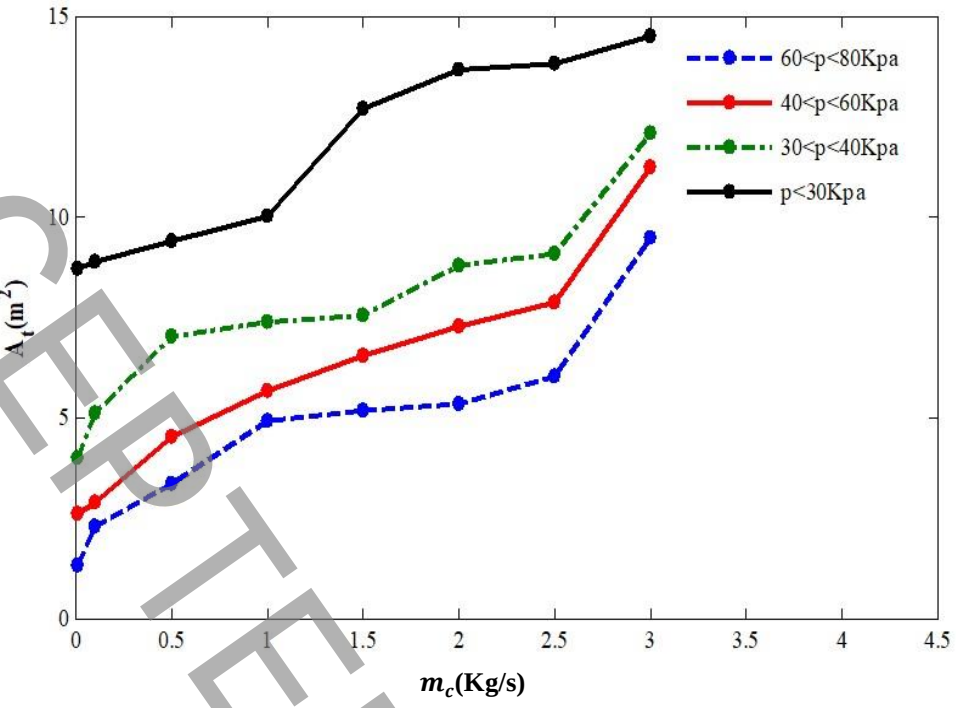

Fig. 11. Effect of working fluid mass rate (R123) on heat exchanger overall area using genetic algorithm

According to optimum data, it is also to be noted that there is a significant fluid mass rate influence on overall heat exchanger area. **Fig. 11** demonstrates that increasing of working fluid mass rate will increase the heat exchanger area (multiplication of one plate area in plate numbers). Additionally, in order to optimize the case in lower pressure drops, the overall area of the heat exchanger will need to increase.

8.2.2. Warm water mass rate influence (hot vapor)

In this section, the warm fluid mass rate influence (heat source) on the genetic algorithm objective function is investigated. It must be noted that geometrical parameters (independent variables) must be assumed to be similar to those considered in the previous section (cold

fluid). By altering the warm fluid mass rate, it is possible to determine its influence on the heat transfer coefficient and overall pressure drop.

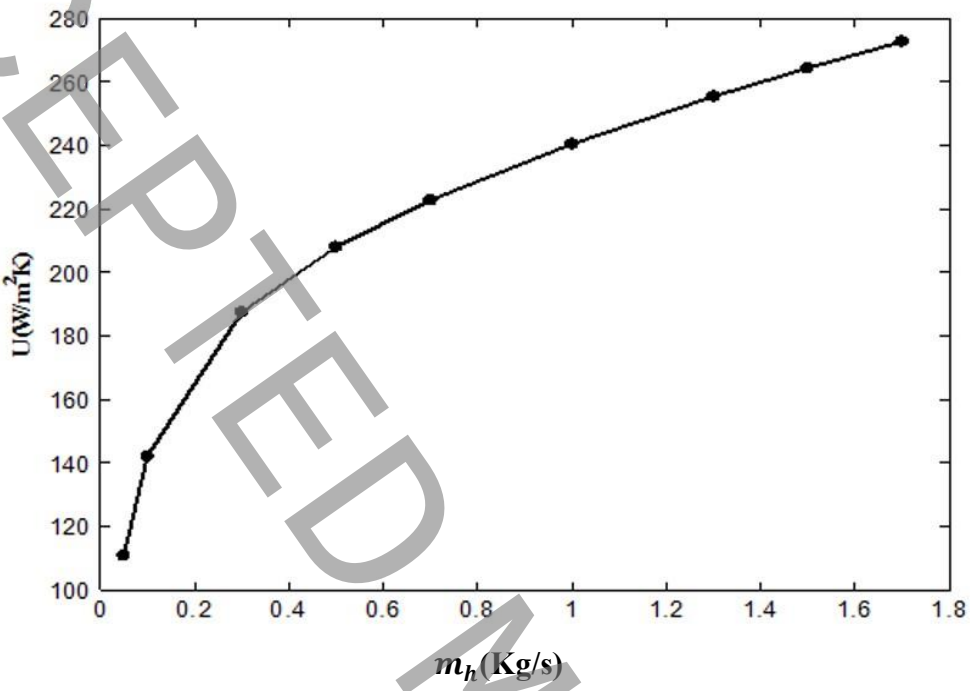

Fig. 12. Hot fluid effect mass rate (hot vapor) on the overall heat transfer coefficient in the evaporator

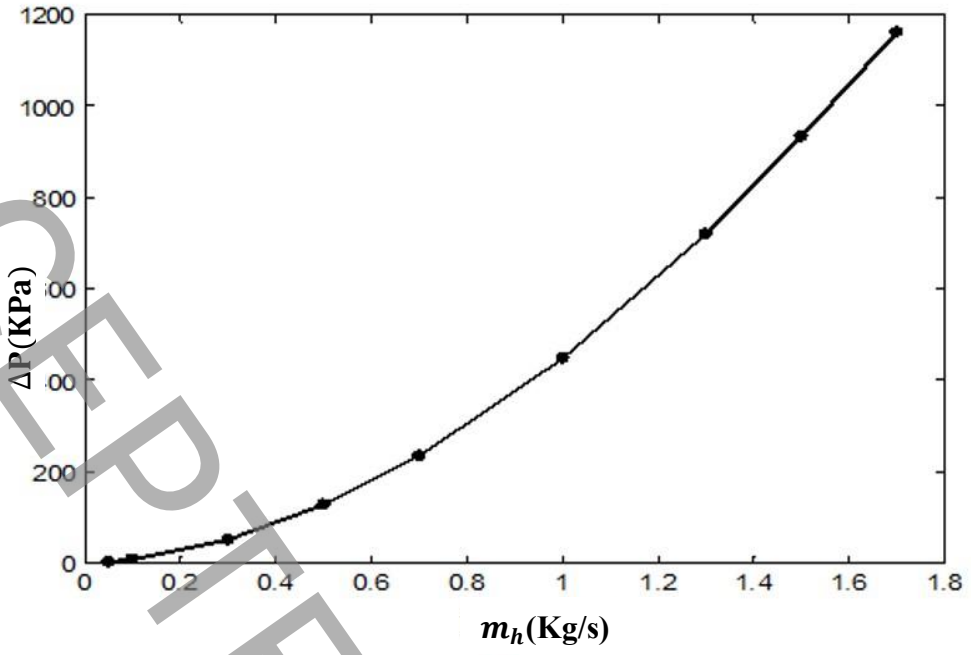

Fig. 13. Hot fluid effect mass rate (hot vapor) on the total pressure drop in evaporator

According to **Fig. 12**, increasing the warm water mass rate will contribute to increasing the overall heat transfer coefficient. The modifications induced are similar to those generated by the cold fluid mass rate. According to Fig. 13, With increasing warm water mass rate, pressure drop will increase considerably as per the thermodynamic flow relations. With higher temperate water, there is greater elevation in pressure drop relative to the cold fluid mass rate case. This indicates that warm fluid mass rate must not exceed a specified value since with high mass rates there is a very high increase in pressure drop relative to heat transfer coefficient which is not appropriate or desirable in heat exchanger design.

Finally, in **Table 7** optimum states for different warm water mass rates (vapor) with vapor as the working fluid medium have been obtained by the genetic algorithm and selected. Inspection of the table reveals that with increasing warm water mass rate both objective functions increase which is more visible in overall pressure drop. For this reason, similarly to

cold mass flow rate, with increasing warm fluid mass rate the number of plates will increase. In this case, the increase in number of plates is greater than the previous state which is more attributable to the overall pressure drop. Therefore, with increasing warm water mass rate, the plate numbers will increase and pressure drop will be reduced to attain the optimum state for heat exchangers. On the other hand, due to the variation of other geometrical parameters, it is evident that with increasing of warm fluid mass rate plate lengths (port vertical distance) will increase. Hence both plate number and port vertical distance contribute to increasing pressure drops. Therefore, to attain pressure drop reduction (as it is in **Table 7**) with increasing warm water mass rate, additional to plate number increasing it can be observed that port horizontal distance (plate width) and also plate diameter will attain their maximum values (0.5,0.15). Plate thickness reduces in order to decrease pressure drop significantly. On the other hand, it must be noted that if fluid mass rate increases then the optimum response range will be more restrained. In higher warm fluid, the plate numbers will reach maximum numbers to prevent high pressure drops. When mass rate is 2 kg/s, pressure drop in the optimum state will reach close to 80kPa indicating that it is not suitable to use higher mass flow rate in heat exchanger design. It can be deduced that variation in warm fluid mass rate has a substantial effect in heat exchanger design and that mass flow rate must not exceed a threshold value. Finally, based on the obtained results, it is apparent that among heat exchanger geometrical parameters, the plates number is the most important one since evidently an increase or decrease in this parameter produces a remarkable variation in the optimization process.

Table. 7. Effect of hot fluid mass rate on heat exchanger optimization using genetic algorithm.

$\dot{m}_h(\frac{\mathbf{kg}}{\mathbf{s}})$	Δp (kPa)	U (W/m^{2}K)	L_h(m)	L_v(m)	t (m)	D_p(m)	N_t
	7.249	121.645	0.190	0.531	0.000747	0.0421	18
0.05	2.745	82.042	0.157	0.612	0.000836	0.0384	25
	1.857	61.851	0.183	0.513	0.000670	0.0541	37
	64.361	428.32	0.15	0.65	0.000997	0.0467	21
0.1	31.892	365.21	0.151	0.679	0.000980	0.0375	27
	7.044	241.99	0.154	0.672	0.000920	0.0625	38
	69.36	367.69	0.342	0.562	0.000675	0.118	31
0.5	37.912	314.548	0.247	0.613	0.000743	0.0968	41
	17.274	276.357	0.189	0.811	0.000849	0.137	53
	73.025	293.67	0.368	0.861	0.000392	0.114	43
1	57.743	174.763	0.412	0.803	0.00411	0.134	56
	77.42	187.84	0.364	0.911	0.000432	0.146	49
1.5	59.841	124.361	0.436	0.899	0.00031	0.15	58
2	77.671	314.91	0.496	0.870	0.00032	0.15	59

9. Conclusions

In this paper, the constraints and conditions for providing optimal states in an ORC plate heat exchanger (PHE) design is considered. Since the inlet pressure of the fluid is 2 bars, the heat exchanger total pressure drop should not be greater than 80 kPa. That is, the choice of optimal conditions must not include pressure drop exceeding 80 kPa. For scenarios where the pressure drop is less than this threshold value, the system achieves a higher heat transfer

coefficient. Regarding to the genetic algorithm optimization calculations, the following results can be obtained:

- By increasing the ports diameter, both the objective function of the overall heat transfer coefficient and total drop is reduced. The alteration in the pressure drop is greater since with increasing port diameter, the flow rate is increased and the fluid velocity decrease which ultimately produces a decrease in pressure drop.
- By increasing the thickness of each plate inside the plate heat exchanger, the two-sheet spacing (flow channel) will naturally be reduced. Eventually, the area of the flow within the channels will be reduced so that the overall heat transfer coefficient and total pressure drop will increase. According to the results presented, the plate thickness should not exceed 0.9m.
- Increasing the horizontal spacing of the ports will increase the area of the plates and eventually increase the average area of the flow channel. As a consequence, both objective functions i.e. total heat transfer coefficient and pressure drop are reduced.
- Increasing the vertical ports space will increase plate areas and ultimately increase the flow area leading to depletion in total heat transfer coefficient. However, unlike the horizontal spacing of the ports, increasing the vertical spacing of the plate heat exchanger results in a increasing the length of the flow path and increasing the frictional pressure drop across the flow channel.
- By increasing the number of heat exchanger plates, both the objective functions i.e. the total heat transfer coefficient and total loss of pressure decrease (the number of flow channels is increased, fluid flow is decelerated and the effective heat transfer surface is increased). This manifests in suppression in both objective functions. Therefore, in the optimal design, it should be noted that with small plates there will be a large drop in pressure. It should also be noted that the number of plates can lead to

more changes in optimization between the design parameters and the variables considered.

- In a fixed design of the heat exchanger, with the increase in the evaporator mass flow rate (R123), both objective functions increase due to an increase of the fluid flow rate to the converter, which is more affected by the pressure drop. Also, by studying the effect of the mass of the fluid on the optimization of the fluid, it was found that the higher the flow rate of the cooler (in order to prevent the excessive drop in the heat exchanger), the number of plates as well as the total area of the heat exchanger increased.
- With the constant consideration of geometric parameters and the increase in hot water flow (thermal source), the objective functions increase. This increase, in particular, is higher in the pressure drop than the cold flow rate, indicating that a large amount of pressure drop occurs in the hot fluid part of the heat exchanger. Also, by studying the effect of hot fluid discharge on the optimization of the heat exchanger, it is evident that with an increase in hot fluid flow, the number of converter plates increases in proportion to the previous mode (the effect of cold flow discharge). Pressure drop at higher fluxes from the hot fluid will increase dramatically and the total area of the heat exchanger will also increase.

Nomenclature

A_1	Effective area, m2	*Re*	Reynolds number
A_{1p}	Projected area, m2	U	Overall heat transfer coefficient, W /(m² K)
b	Mean flow channel gap, m	$\dot{q}$	heat flux, Wm^{-2}

c_p	Specific heat of fluid, J kg^{-1} K^{-1}
D_e	Channel equivalent diameter, m
D_p	Port diameter, m
fr	Friction factor
G	Mass flux velocity, kg m^{-2} s^{-1}
h	Heat transfer coefficient, W m^{-2} K^{-1}
k_w	Thermal conductivity
L_c	Total length of compact plates, m
L_{eef}	Effective length of the flow, m
L_h	Horizontal distance of ports, m
L_v	Vertical distance of ports, m
L_w	Effective plate width, m
N_{cp}	Number of channels per pass
N_p	Number of passes
N_t	Total number of plates
P	Plate depth, m
Δp	Pressure drop, kPa
t	Plate thickness, m
γ	latent heat, J kg^{-1}
ρ	Density, kg m^{-3}
μ	Viscosity, N m-1 s-1
$\emptyset$	Enlargement factor
$\dot{q}$	heat flux, Wm^{-2}
γ	latent heat, J kg^{-1}

Subscripts

c	Cold fluid
ch	Channel
eq	equivalent
f	fluid
h	Hot fluid
sp	single phase
tot	total
tp	two phase
p	Port

References

[1] W. Colella, Design options for achieving a rapidly variable heat-to-power ratio in a combined heat and power (CHP) fuel cell system (FCS), Journal of Power Sources, 106(1-2) (2002) 388-396.
[2] G.L. Basso, B. Nastasi, F. Salata, I. Golasi, Energy retrofitting of residential buildings—How to couple Combined Heat and Power (CHP) and Heat Pump (HP) for thermal management and off-design operation, Energy and Buildings, 151 (2017) 293-305.
[3] J. Keirstead, N. Samsatli, N. Shah, C. Weber, The impact of CHP (combined heat and power) planning restrictions on the efficiency of urban energy systems, Energy, 41(1) (2012) 93-103.
[4] K.K. Shah, A.S. Mundada, J.M. Pearce, Performance of US hybrid distributed energy systems: Solar photovoltaic, battery and combined heat and power, Energy Conversion and Management, 105 (2015) 71-80.
[5] F. Vélez, J.J. Segovia, M.C. Martín, G. Antolín, F. Chejne, A. Quijano, A technical, economical and market review of organic Rankine cycles for the conversion of low-grade heat for power generation, Renewable and Sustainable Energy Reviews, 16(6) (2012) 4175-4189.
[6] J. Wang, L. Zhao, X. Wang, An experimental study on the recuperative low temperature solar Rankine cycle using R245fa, Applied Energy, 94 (2012) 34-40.
[7] N.B. Desai, S. Bandyopadhyay, Process integration of organic Rankine cycle, Energy, 34(10) (2009) 1674-1686.
[8] J. Xu, X. Luo, Y. Chen, S. Mo, Multi-criteria design optimization and screening of heat exchangers for a subcritical ORC, Energy Procedia, 75 (2015) 1639-1645.
[9] M.-H. Yang, R.-H. Yeh, Economic performances optimization of the transcritical Rankine cycle systems in geothermal application, Energy Conversion and Management, 95 (2015) 20-31.
[10] M.-H. Yang, R.-H. Yeh, Economic performances optimization of an organic Rankine cycle system with lower global warming potential working fluids in geothermal application, Renewable Energy, 85 (2016) 1201-1213.
[11] A.I. Papadopoulos, M. Stijepovic, P. Linke, On the systematic design and selection of optimal working fluids for Organic Rankine Cycles, Applied thermal engineering, 30(6-7) (2010) 760-769.
[12] Y. Dai, J. Wang, L. Gao, Parametric optimization and comparative study of organic Rankine cycle (ORC) for low grade waste heat recovery, Energy Conversion and Management, 50(3) (2009) 576-582.
[13] J. Sarkar, S. Bhattacharyya, Potential of organic Rankine cycle technology in India: working fluid selection and feasibility study, Energy, 90 (2015) 1618-1625.
[14] T. Deethayat, T. Kiatsiriroat, C. Thawonngamyingsakul, Performance analysis of an organic Rankine cycle with internal heat exchanger having zeotropic working fluid, Case Studies in Thermal Engineering, 6 (2015) 155-161.
[15] S. Aghahosseini, I. Dincer, Comparative performance analysis of low-temperature Organic Rankine Cycle (ORC) using pure and zeotropic working fluids, Applied Thermal Engineering, 54(1) (2013) 35-42.
[16] T. Hung, S. Wang, C. Kuo, B. Pei, K. Tsai, A study of organic working fluids on system efficiency of an ORC using low-grade energy sources, Energy, 35(3) (2010) 1403-1411.
[17] M. Ibarra, A. Rovira, D.-C. Alarcón-Padilla, J. Blanco, Performance of a 5 kWe Organic Rankine Cycle at part-load operation, Applied energy, 120 (2014) 147-158.
[18] J. Roy, A. Misra, Parametric optimization and performance analysis of a regenerative Organic Rankine Cycle using R-123 for waste heat recovery, Energy, 39(1) (2012) 227-235.
[19] Z. Wang, N. Zhou, J. Guo, X. Wang, Fluid selection and parametric optimization of organic Rankine cycle using low temperature waste heat, Energy, 40(1) (2012) 107-115.
[20] P.J. Mago, L.M. Chamra, K. Srinivasan, C. Somayaji, An examination of regenerative organic Rankine cycles using dry fluids, Applied thermal engineering, 28(8-9) (2008) 998-1007.
[21] M. Yari, Performance analysis of the different organic Rankine cycles (ORCs) using dry fluids, International Journal of Exergy, 6(3) (2009) 323-342.
[22] H. Chen, D.Y. Goswami, E.K. Stefanakos, A review of thermodynamic cycles and working fluids for the conversion of low-grade heat, Renewable and sustainable energy reviews, 14(9) (2010) 3059-3067.

[23] J. Roy, M. Mishra, A. Misra, Performance analysis of an Organic Rankine Cycle with superheating under different heat source temperature conditions, Applied Energy, 88(9) (2011) 2995-3004.
[24] L. Wang, B. Sunden, Optimal design of plate heat exchangers with and without pressure drop specifications, Applied Thermal Engineering, 23(3) (2003) 295-311.
[25] S. Karellas, A. Schuster, A.-D. Leontaritis, Influence of supercritical ORC parameters on plate heat exchanger design, Applied Thermal Engineering, 33 (2012) 70-76.
[26] Y.-Y. Yan, T.-F. Lin, Evaporation heat transfer and pressure drop of refrigerant R-134a in a plate heat exchanger, (1999).
[27] S.A. Vaziri, M. Ghannad, O.A. Bég, Exact thermoelastic analysis of a thick cylindrical functionally graded material shell under unsteady heating using first order shear deformation theory, Heat Transfer—Asian Research, 48(5) (2019) 1737-1760.
[28] D. Walraven, B. Laenen, W. D'haeseleer, Comparison of shell-and-tube with plate heat exchangers for the use in low-temperature organic Rankine cycles, Energy conversion and management, 87 (2014) 227-237.
[29] J.H. Holland, Adaptation in natural and artificial systems: an introductory analysis with applications to biology, control, and artificial intelligence, MIT press, 1992.
[30] K. Deb, Optimization for engineering design: Algorithms and examples, PHI Learning Pvt. Ltd., 2012.
[31] H. Najafi, B. Najafi, P. Hoseinpoori, Energy and cost optimization of a plate and fin heat exchanger using genetic algorithm, Applied Thermal Engineering, 31(10) (2011) 1839-1847.
[32] J.G. Andreasen, U. Larsen, T. Knudsen, L. Pierobon, F. Haglind, Selection and optimization of pure and mixed working fluids for low grade heat utilization using organic Rankine cycles, Energy, 73 (2014) 204-213.
[33] H. Xi, M.-J. Li, C. Xu, Y.-L. He, Parametric optimization of regenerative organic Rankine cycle (ORC) for low grade waste heat recovery using genetic algorithm, Energy, 58 (2013) 473-482.
[34] J. Wang, M. Wang, M. Li, J. Xia, Y. Dai, Multi-objective optimization design of condenser in an organic Rankine cycle for low grade waste heat recovery using evolutionary algorithm, International communications in heat and mass transfer, 45 (2013) 47-54.
[35] R. Hilbert, G. Janiga, R. Baron, D. Thévenin, Multi-objective shape optimization of a heat exchanger using parallel genetic algorithms, International Journal of Heat and Mass Transfer, 49(15-16) (2006) 2567-2577.
[36] H. Najafi, B. Najafi, Multi-objective optimization of a plate and frame heat exchanger via genetic algorithm, Heat and mass transfer, 46(6) (2010) 639-647.
[37] M. Rashidi, O.A. Bég, A.B. Parsa, F. Nazari, Analysis and optimization of a transcritical power cycle with regenerator using artificial neural networks and genetic algorithms, Proceedings of the Institution of Mechanical Engineers, Part A: Journal of Power and Energy, 225(6) (2011) 701-717.
[38] O. Anwar Beg, M. Rashidi, N. Mehr, Comparative thermodynamic study of air standard cycles with heat transfer and variable specific heats of the working fluid, Int. J. Appl. Math. and Mech, 10(2) (2014) 41-60.
[39] H. Martin, Heat exchangers, CRC Press, 1992.
[40] H. Martin, A theoretical approach to predict the performance of chevron-type plate heat exchangers, Chemical Engineering and Processing: Process Intensification, 35(4) (1996) 301-310.
[41] D.-H. Han, K.-J. Lee, Y.-H. Kim, Experiments on the characteristics of evaporation of R410A in brazed plate heat exchangers with different geometric configurations, Applied thermal engineering, 23(10) (2003) 1209-1225.
[42] M. Mitchell, An introduction to genetic algorithms, MIT press, 1998.
[43] S. Kakac, H. Liu, A. Pramuanjaroenkij, Heat exchangers: selection, rating, and thermal design, CRC press, 2020.